(7) Doi, M.; Edwards, S. F. *J. Chem. Soc., Faraday Trans. 2* **1978**, *74*, 1789.
(8) Doi, M.; Edwards, S. F. *J. Chem. Soc., Faraday Trans. 2* **1978**, *74*, 1802, 1818.
(9) Doi, M.; Edwards, S. F. *J. Chem. Soc., Faraday Trans. 2* **1979**, *75*, 38.
(10) James, H. M.; Guth, E. *J. Chem. Phys.* **1943**, *11*, 455.
(11) Gee, Herbert; Roberts *Polymer* **1969**, *6*, 541.
(12) Yen; Eichinger *J. Polym. Sci., Polym. Phys. Ed.* **1978**, *16*, 121.
(13) Flory, P. J. *Macromolecules* **1979**, *12*, 119.
(14) Collins, P. D. B. "Regge Theory and High Energy Physics"; CUP 1977, p 64.
(15) de Gennes, P.-G. *Phys. Lett. A* **1972**, *38*, 339.
(16) Titchmarsh, E. C. "Theory of Functions", CUP 1939, 186.

Graph-Like State of Matter. 14. Statistical Thermodynamics of Semidilute Polymer Solution

P. Irvine and M. Gordon*

Department of Chemistry, University of Essex, Wivenhoe Park, Colchester CO4 3SQ, England. *Received December 31, 1979*

ABSTRACT: The phase equilibrium behavior of solutions of polystyrene in cyclohexane, covering broad neighborhoods of their critical points, is well-described by a pseudo-two-phase "bridging" theory. This theory retains the essential contribution of athermal Poisson statistics of the original version by Koningsveld, Stockmayer, Kennedy, and Kleintjens. However, the theory has been substantially simplified and amends the Flory–Huggins model along the lines suggested by its originators. Neither the mean-field character nor the implicit status of a nonlocalized model is abandoned. Indeed, the *translational* partition function of the original model is the only part amended, in order to differentiate the behavior of polymer chains in the "dilute" and "concentrated" pseudophases. Although the differential effect between the two phases is minute, of order kT per polymer chain, it reproduces well the expected transitional behavior around the concentration ϕ^* (entanglement point). The correction, reinforced by the Huggins second-nearest-neighbor correction, drastically changes the theoretical virial series and produces the shapes of spinodal and cloud point curves which are indeed observed. The model is fitted to extensive spinodal data by pulse-induced critical scattering (PICS), to cloud points, and to critical points. The effects of polydispersity are nicely reproduced by the theory. The strategy of validating models through successive refinements is briefly discussed. Further refinement of the statistical mechanical mean-field theory of nonpolar polymer solutions around their critical points now hinges on the production of test samples more accurately characterized than at present with respect to molecular weight.

The problem of refining statistical-thermodynamic models of the free energy ΔG of mixing of a polymer solution, the basic function from which all its thermodynamic properties flow, exemplifies the kind of vicious circle which frequently challenges physical science. It is not that we lack experimental techniques of sufficient sensitivity: simple experiments contain an enormous wealth of information. But unfortunately we need to be in possession of an excellent free energy function already if we are to be able to extract that information unambiguously. To exploit highly sensitive thermodynamic measurements requires exceedingly well-characterized polymer samples, but such characterization requires prior knowledge of the thermodynamics. For an example at a low level: ΔG depends on $\bar{M}_n$, the number-average molecular weight, but the search for precision in $\bar{M}_n$ founders on the effects of higher virial coefficients on the requisite extrapolation if pressed too far.

The strategy to be adopted for breaking such a vicious circle has been well formulated by Bachelard[1] in a passage which may be translated: "As the application (i.e., of theory) is submitted to successive approximations, one may say that the scientific concept corresponding to a particular phenomenon is the *pattern* of well-ordered successive approximations. Scientific conceptualization needs a series of concepts progressing toward perfection in order to realize the dynamism we aim at, to serve as a fulcrum for inventive ideas." In the present case, the pattern of orderly progression is clear. Refinement of ΔG and the characterization of polymers must work in close harmony, as near as possible between the unknown domain and what is firmly established. The next experiment to develop is dictated by the next most sensitive physical quantity measurable which the current state of the statistical-mechanical theory can just embrace. It would be counterproductive to tackle the highly sensitive properties straight away. If we did, we would be forced to fit several unknown parameters all at once. Even if we guessed their relative importance correctly, the set of parameters obtained by optimization will be vitiated by statistical coupling within the set. Only at the interface between the known and the unknown can we hope to introduce one parameter at a time. This is the correct procedure, which allows the circle to be broken by constant feedback between characterization and refinement.

Successive Refinements of ΔG

It will emerge that the pattern of well-ordered successive approximations coincides neither with the historical order in which they have been proposed nor with the sequence based on decreasing absolute magnitudes of changes induced in ΔG itself. A small change in ΔG may be reflected in a large change of a derived quantity like a spinodal.

The correct sequence, in the absence of adjustable parameters, is in decreasing fractional changes in the variance σ^2 of the relevant optimization in fitting data. The absence of adjustable parameters is an ideal not fully attainable; one adjustable parameter is present in the original Flory–Huggins model, and a second was introduced soon after (β_0 and β_1 below). Thereafter, three more parameters are associated with four of the succeeding refinements selected for testing in this work, but all three have molecular significance which suggests restrictions to their adjustments within narrow ranges.

0024-9297/80/2213-0761$01.00/0

Let R be the gas constant, T the absolute temperature, and ϕ_i the volume fraction of component i with molecular chain length m_i defined by

$$m_i = M_i/c \tag{1}$$

where M_i is the molecular weight and

$$c = \text{mol wt of solvent} \times \frac{\text{specific vol of solvent}}{\text{specific vol of polymer}} \tag{2}$$

For the system polystyrene (PS)/cyclohexane (CH), c = (84.16 × 1.300)/0.929 = 117.76. The overall volume fraction of polymer is denoted by $\phi = \sum_1^N \phi_i$.

Accordingly, the solvent may be assigned subscript 0 and $m_0 = 1$. It is customary to define

$$\Gamma = (\Delta G/RT) - \sum_0^N \phi_i m_i^{-1} \ln \phi_i \quad (\text{usually } N \to \infty) \tag{3}$$

The original Flory–Huggins[2,3] model took the form

$$\Gamma_4 = (\beta_1/T)\phi_0\phi \qquad \phi_0 \equiv 1 - \phi \tag{4}$$

Later it was amended to

$$\Gamma_5 = (\beta_0 + \beta_1/T)\phi_0\phi \tag{5}$$

In 1957, Orofino and Flory[4] introduced a further correction and parameter γ, whose importance[5] had not been recognized in the original theory. Combining it with (5) this takes the form

$$\Gamma_6 = [(\beta_0 + \beta_1/T)/(1 - \gamma\phi)]\phi_0\phi \tag{6}$$

One of the subsequent attempts[7] to improve the theory by "bridging" between concentrated and dilute solution in the intermediate concentration range was directly aimed at fitting phase equilibrium data. The free-energy function, when adapted to polydisperse samples by crude preaveraging, reads (after putting the original[7] parameter α equal to 0):

$$\Gamma_7 = \Gamma_6 + \phi_0\phi(\exp[-\lambda\bar{m}_w^{1/2}\phi])[2^{-1} - (1 - \gamma)(\beta_0 + \beta_1T^{-1})](1 + \lambda_0\bar{m}_w^{1/2})^{-1}[1 - (1.748(2^{-1} - (1 - \gamma)(\beta_0 + \beta_1T))\bar{m}_w^{1/2})^{-1}] \ln [1 + 1.748(2^{-1} - (1 - \gamma) \times (\beta_0 + \beta_1T^{-1}))\bar{m}_w^{1/2}] \tag{7}$$

The preaveraging here uses the approximation

$$\sum_1^N \phi_i m_i^{1/2} \simeq (\sum_1^N \phi_i m_i)^{1/2} \equiv \phi\bar{m}_w^{1/2} \tag{8}$$

where $\bar{m}_w$ is the weight average molecular chain length. The present work replaces (7) by a simpler equation containing a temperature-independent correction to Γ_6 and a new heterodispersity parameter α (cf. eq 18 below):

$$\Gamma_9 = \Gamma_6 + \phi_0\sum_{i=1}^N \phi_i m_i^{-1} \exp[-\lambda_0\sum_{j=1}^N \phi_j m_j^{-1}(m_i^{1/2} + m_j^{1/2})^3] \times [1 - \alpha \ln (m_i/\langle m_i\rangle_{geom})] \tag{9}$$

where $\langle\ \rangle_{geom}$ means the geometric mean.

The model underlying this equation is presented in section III. It is found, moreover, that the progression in order of decreasing σ^2 (see later, Table I and section IV) calls for implementation of the second-nearest-neighbor approximation in the combinatorial entropy. This correction was deduced as early as 1942 by Huggins,[3] and it translates into the following function of ϕ:

$$\Gamma = \Gamma_9 + [(1 - \gamma)\phi \ln (1 - \gamma) - (1 - \gamma\phi) \ln (1 - \gamma\phi)]\gamma^{-1} \tag{10}$$

II. Thermodynamic Measurements

1. **Survey of Measurable Quantities.** ΔG functions like those in the last section are not directly measurable, and polydispersity of test samples has dominated the refinement by using derived thermodynamic quantities. This calls for a list of thermodynamic measurables in an approximate order of increasing sensitivity to experimental variables (especially to polydispersity): (i) colligative properties, (ii) spinodals, (iii) critical points, (iv) cloud points and phase-volume ratios, and (v) second virial coefficients and partition coefficients (Breitenbach–Wolf plots).

Colligative properties (osmotic pressure etc.) were the prime arms with which the Flory–Huggins theory rose to fame. Proceeding down the list of properties, more detailed and specific interactions between polymer molecules tend to come into play. This process culminates in the nonlinear dependence of partition coefficients on molecular weight in Breitenbach–Wolf[6] plots.

It became clear in the middle sixties that spinodals could be most attractive to supplement the classical exploration of colligative properties. Spinodals are *relatively* easy to compute but were thought in 1968 to be nonmeasurable by Koningsveld and held to be of questionable existence by Fisher et al.[9] Nevertheless, the first spinodal measurements were made soon after by Scholte[10] in Koningsveld's laboratory! Simultaneously, much improved apparatus was developed for spinodal measurements by thermal stepping (pulse-induced critical scattering or PICS).[11] Paradoxically, cloud points are more easily and precisely measured, and therefore abundant in the literature, but they are hard to compute in practice for polydisperse samples. In this work, we calculate the parameters for a global optimization of the spinodal derived from the free-energy functions in section I over extensive data (section V) and test the parameters for (10) by proceeding down the list of properties to critical points and cloud points, measured in other laboratories as well as ours. All the data are for polystyrene/cyclohexane (PS/CH), the best-documented system.

Analytical expressions for the spinodals (ϕ_{sp}, T_{sp}) of the simpler ΔG functions (eq 4–7) have been derived directly from the Gibbs condition[12]

$$J \equiv J(\phi_{sp}, T_{sp}) = \text{Det } [\partial^2\Delta G/\partial\phi_i\,\partial\phi_j] = 0 \tag{11}$$

For monodisperse solutions, even (9) and (10) have analytical solutions. However, recently simpler methods of computing spinodals[13] from the moments of the molecular weight distribution (*mwd*) have been developed.[5,14] We define the kth moment by

$$M_k = \sum_1^N \phi_i m_i^k \tag{12}$$

so that $\phi = M_0$, $\bar{M}_w = M_1/M_0$, $\bar{M}_z = M_2/M_1$, etc. Because of a truncation theorem,[13] the free-energy functions listed, except (9) and (10), lead to spinodals dependent on a small set of moments. In such cases, no explicit spinodal equation is required. Instead, the MWD of practically an infinite number of components can be strictly replaced[5] by an "r-equivalent" MWD with $\lceil r/2 \rceil$ delta-function components. Here $\lceil r/2 \rceil$ means the smallest integer $\geq r/2$. The determinant J reduces to order $\lceil r/2 \rceil$, and its roots are found on the computer by eigenvalue methods. For the ΔG functions eq 4–6, a single component suffices, and for (7) two components are needed. For (10) the theorem predicts no exact truncation. However, we are still content to replace the MWD of the actual test sample by those of notional mixtures of two delta functions, selected in each case to reproduce *exactly* the estimates of $\bar{M}_w$, $\bar{M}_z$, $\bar{M}_{z+1}$ (or equivalently, M_1, M_2, M_3). The truncation proves successful, and there is no point, at the present state of

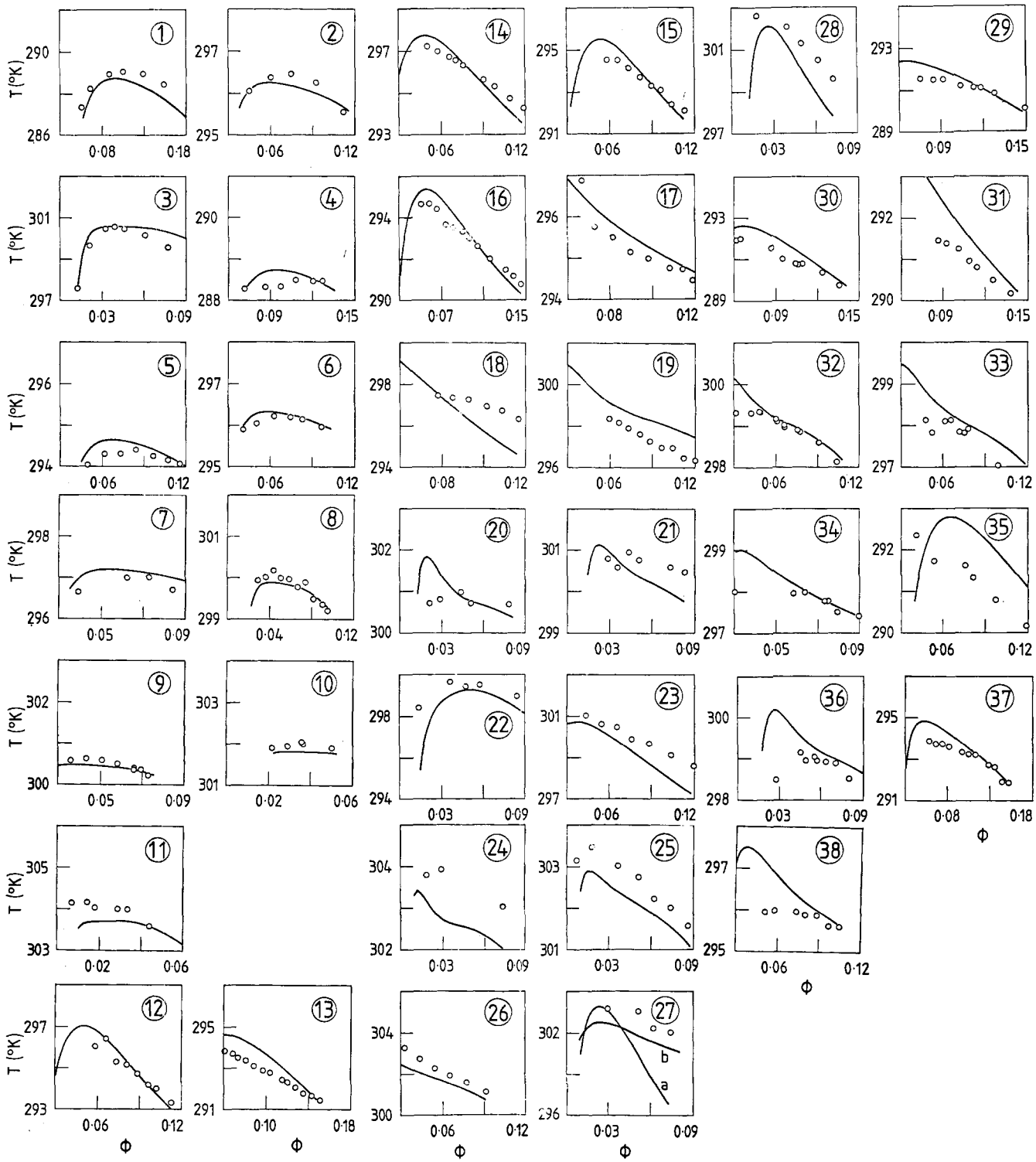

Figure 1. Fittings of measured spinodal points for samples (Table II) shown by plot numbers of polystyrene in cyclohexane to curves computed from eq 10. Samples 1–11 were treated as sharp fractions of molecular weight given by $\bar{M}_w$ in Table II. Parameters found by optimization (row 3 of Table IB) were $\beta_0 = 0.1717$, $\beta_1 = 100.53$, $\gamma = 0.4651$, $\lambda_0 = 0.6215$, $\alpha = 0.031$. For plots 27a and 27b see text and Table III.

development of molecular weight measurements, in including estimates of higher moments. Detailed computational procedures are reserved for another paper,[14] which will describe the computation of properties ii–iv generally.

2. Validation of Measurements and Model Theories. The efficient extraction of information from phase equilibrium experiments comprises two aspects which overlap to some extent. On the one hand the assessment of error bounds in the measured quantities should be based on the right criteria; on the other, the merits of rival model concepts can be usefully compared on the basis of error statistics only in the proper context of explicit principles of inductive inference.

The use of standard deviations σ, or variances σ^2, in measuring errors in optimized fits of data to theories is of course standard. The choice of variable in least-squares fittings is, however, unusually important in this work. The phase diagrams (Figure 1) lie in the (ϕ,T) plane. A sealed cell of solution with fixed ϕ returns slightly different values of T_{sp} on replicate measurements, and it might seem that

thermometry is less precise than measurements of concentration. It might thus appear natural to optimize by minimizing the quantity

$$S_T = \sum_1^p (T_{sp(calcd)} - T_{sp(exptl)})^2 \quad (13)$$

p is the number of data points. Not only does this prove computationally forbidding, but it is actually appropriate to minimize instead

$$S = \sum_1^p (J_{(calcd)} - J_{(exptl)})^2/RT = \sum_1^p J_{(calcd)}{}^2/RT \quad (14)$$

where

$$J_{(calcd)} = J_{(calcd)}(\phi_{sp(exptl)}, T_{sp(exptl)}) \quad (15)$$

and $J_{(exptl)}$, the "true" value of the spinodal determinant at the measured spinodal data point, has, by definition, been set equal to zero in (14). The first reason for preferring (14) to (13) is that, through the Debye–Scholte[15] plot T_{sp} is found experimentally by extrapolation of the reciprocal intensity I^{-1} of scattering against T, and $I^{-1} \propto J$; accordingly relative errors in spinodal temperatures are proportional to those in J and not directly proportional to errors in thermometry. Secondly the loci $T_{sp} = T_{sp}(\phi_{sp})$ comprise curves passing, according to quite general thermodynamic principles, from almost horizontal to almost vertical course over small ranges of ϕ (experimentally this is seen in Figure 1, plot 3). The relative errors in thermometry do dominate the near-horizontal range, and those in ϕ the near-vertical portions, so that neither of these two variables alone furnishes a suitable variance for testing models. A better solution is to minimize the variance of the distance of measured points (ϕ_{sp}, T_{sp}) from the theoretical curve at *right angles* to the curve (rather than in a vertical or horizontal direction). This goal is closely approached by the variance of J, since the calculated contour lines of J near the theoretical spinodal curve $J = 0$ are found to follow almost parallel courses in the (ϕ, T) plane over the range of scatter of experimental points. Once the parameters have been found by minimizing σ^2, they are used to calculate theoretical spinodal temperatures for given $\phi_{sp(exptl)}$ by computing the temperature for which an eigenvalue of J vanishes.

III. Improved Bridging-Theory Model Underlying Equation 9

Flory[16] drew attention in 1945 to the breakdown of the original Flory–Huggins model in the range of dilute solutions. He pointed to what amounts to a *statistical heterogeneity* of such solutions; some chains become isolated from all others, and consequently their segments no longer "see" the average environment assumed to apply to all segments. In 1974, Koningsveld, Stockmayer, Kennedy, and Kleintjens[7] proposed a two-phase model to allow for this heterogeneity. Of course, a two-phase model implies the use of two different partition functions for the polymer. Accordingly, these authors chose to assign different ΔG functions for *chain segments* in overlapped or nonoverlapped coil domains, respectively. The choice of segments, and of second-virial theory, as the framework for constructing their bridging model was quite natural. Despite the extensive literature on solutions containing chains isolated at high dilution, no useable partition function was then available for such a chain as a whole. Second-virial theory amounts to exploring the state of one chain indirectly through the approach of another.

A single-chain partition function was given in 1977 in part IX of this series.[17] It was quite simply based on the self-intersecting random walk, yet allowed the thermal expansion of a chain to be successfully modeled, both by fitting light-scattering data and through the crude rederivation of Flory's[18] equation ($\alpha^5 - \alpha^3 = km^{1/2}$). An attempt at injecting the new partition function for an isolated chain into the bridging model proposed here leads to some embarrassment. It emerges that the Flory–Huggins model already implicitly assigns the same function, as least to the approximation required here, to a chain at infinite dilution! But this is not really surprising: the Flory–Huggins model makes no provision for excluding self-intersection (cf. Staverman[19]). Accordingly, no correction seems due for statistical heterogeneity with respect to the conformational partition function of a self-intersecting chain.

However, a deeper look reveals that a correction of the bridging type, using a two-phase model, is still called for in the translational part of the chain partition function. We retain the athermal Poisson statistics of the original bridging theory,[7] now applied to chains rather than segments. Equally, we retain the assignment of the uncorrected (high-concentration) partition function (or ΔG) applicable to chains which overlap others and assume chain dimensions are unaffected by changes in ϕ and T (see section V.5). The effect of the translational correction is simply to introduce a term RT into the free energy, or a factor exp(−1) into the partition function, of each *isolated* chain.

1. The Factor exp(−1). The partition function of a chain can, in the Flory–Huggins model, be split into a conformational and a translational factor (cf. Flory[20]). There is no restriction placed specifically on self-intersection of a chain in the derivation of the model, so that the conformational factor is essentially that of a freely intersecting chain. Thus consider the limit at infinite dilution at the Θ point.

$$\lim_{\phi \to 0} (Z_N{}^{1/N}) = \binom{n_0 + Nr}{N}^{1/N} z(z-1)^{r-2}$$

$$\xrightarrow[\text{approximation}]{\text{Stirling}} = [(n_0 + Nr)e/N] z(z-1)^{r-2} \quad (16)$$

Here Z_N is the absolute Flory–Huggins configurational partition function for N chains, each occupying r contiguous sites, placed together with n_0 solvent molecules on a lattice of $(n_0 + Nr)$ sites. The binomial coefficient in (16) is the translational term, the number of ways of placing the first segment of each chain. The factor $z(z-1)^{r-2}$ is the conformational factor, the number of ways of placing the remaining segments of a freely intersecting chain on the lattice graph. (More strictly one might regard the factor z as the rotational term and $(z-1)^{r-2}$ as the conformational one.) Also consider the bulk limit:

$$\lim_{\phi \to 0} (Z_N{}^{1/N}) = \binom{Nr}{N}^{1/N} z(z-1)^{r-2} \exp(-r) \quad (17)$$

Recall from Poisson statistics that if a large number S of objects is placed randomly in S boxes, the chance that one object is the sole occupant of its box is exp(−1). Accordingly, in (17), the binomial coefficient is the translational factor of placing the first segment as before, $z(z-1)^{r-2}$ is the conformational factor as before, but $\exp(-rN)$ occurs as a factor in Z_N, being the estimate for the fraction of configurations for which each of the $S = rN$ segments is in sole occupancy of its lattice site. (A small fraction of the multiple segment occupancies thus discounted would be self-intersections of the chain.)

The classical Flory–Huggins model also assigns implicitly a partition function $Z = Z_N{}^{1/N}$ per chain at the Θ point in the finite concentration range between the asymptotic

limits in eq 16 and 17. The translational factor, the binomial coefficient term

$$\binom{n_0 + Nr}{N}^{1/N}$$

is valid throughout the concentration range (in the bulk limit the number of solvent molecules n_0 is zero). The conformational factor $z(z-1)^{r-2}$ is equally valid throughout for a freely intersecting ("phantom") chain. Accordingly, as we gradually dilute the polymer from bulk toward infinite dilution, the whole effect is modeled by the gradual increase from $\exp(-r)$ (eq 17) to unity (eq 16) of the factor representing essentially the gradual increase of allowable configurations as the chains are spaced out from each other in the solvent, thus abolishing the intermolecular excluded-volume effect.

The Flory–Huggins model, without further correction, portrays the Θ point and phase separation below the Θ temperature as is well known, and the correction to be made by a bridging theory in the transitional concentration region of statistical heterogeneity will be a small one. Phase separation in the unstable neighborhood of the critical point will be foreshadowed in its stable and metastable neighborhoods by the applicability of the approximate two-phase model. The two pseudophases in this region will have partition functions which differ only by a small factor, but one that amply affects sensitive features in the free energy landscape, like phase boundaries, which depend on higher derivatives of the free energy ΔG of mixing.

To determine this appropriate small factor, consider the Stirling limit for the translational term shown in square brackets in (16). The factor $(n_0 + N_r)/N$ counts the number of lattice sites available on average for the first segment of a chain. Instead of thinking of this as an average, let us allocate a distinct box of this number of sites to each chain to be placed on the overall lattice of N such boxes. Then the remaining factor, $\exp(1)$, in the square bracket mediates the final gradual elimination of the interchain excluded volume effect as we approach infinite dilution. It signifies that the Flory–Huggins model does *not* place each chain in a separate box, but that by Poisson statistics there will be fluctuations about the average of one chain per box. (As above, the chance that a chain is the sole occupant of a given box is $\exp(-1)$.) Of course, when we approach infinite dilution, each box becomes very large, and even the presence of several chains in a box will ultimately lead to a negligible chance of their coils overlapping. The effect of the factor $\exp(1)$ in $Z_N^{1/N}$ then gradually becomes negligible.

The smooth averaging by the Flory–Huggins model of the disappearance of the effects of chain overlap in the transitional concentration range, long before infinite dilution is approached, is just what requires correction by the bridging theory. Once a chain is separated from overlaps with other chains by dilution, its partition function should (as a crude approximation) jump to its effective limiting form for a separated chain. A finite fraction of nonoverlapping chains exists in the transitional concentration region. The partition function of such a chain should be corrected as if it were already in a box by itself, rather than allowing its overlaps to be reduced gradually by further dilution as implied by the uncorrected Flory–Huggins model. We see that the partition function of a chain, which on dilution moves into the fraction P of isolated chains, should be reduced at a stroke by a factor $\exp(-1)$. In this way a rough correction is made for the onset of the statistical heterogeneity which Flory recognized as a source of error. Fortunately this factor $\exp(-1)$ is seen to derive not from the approximate configurational partition function of the Flory–Huggins model, but merely from the correct translational factor present in any theory. The factor $\exp(-1)$ is conceptually related to the same factor said to give rise to the "communal entropy" in cell theories for liquids,[21] or for fusion:[22] the effect of the correction is equivalent in the present case to removing two degrees of freedom from the share of an isolated chain in the equipartition energy.

2. Generalization to Polydisperse Polymers. The obvious generalization of the treatment in the last section would multiply by $\exp(-1)$ the partition function of every chain, irrespective of its chain length, whose coil does not overlap any other. This obvious generalization does well near a critical point, but much better overall fits are presented below for the following further generalization, in which $\exp(-1)$ is replaced, for chain length m_i, by:

$$R_i \equiv \exp(-1)[m_i/(\prod_{k=1}^{N^*} m_k)^{1/N^*}]^{\alpha} \tag{18}$$

N^* is the total number of distinct chain lengths.

Here α is a semiempirical parameter, and for $\alpha = 0$ we return to the simple case just outlined. Moreover, for monodisperse samples, R_i also reverts to $\exp(-1)$ irrespective of the value of α. Finally, the form of R_i is dictated by the postulate that the factors for chains of different m are coupled through a geometric mean rule, so that

$$(\prod_{i=1}^{N^*} R_i)^{1/N^*} = \exp(-1) \tag{19}$$

The physical meaning of α is intended to cover a variety of possible effects and is discussed in section IV.4. The fact that we are still merely amending the translational partition function suggests that coupling between R_i's should be weak. The fitting of experimental data does indeed lead to optimized values of α as low as about 0.03 (Table IB).

The use of the correction factors R_i in the partition function also requires calculation of the fraction P_i of the chains of length m_i in the systems which are isolated (i.e., nonoverlapping). From Poisson statistics applied to polydisperse random freely-interpenetrating spheres, we have

$$P_i = \exp[-\lambda_0 \sum_{j=1}^{N^*} \phi_j m_j^{-1}(m_i^{1/2} + m_j^{1/2})^3] \tag{20}$$

This replaces eq 12 of Koningsveld et al.[7] for the monodisperse case ($N^* = 1, i = 1$). Accordingly, the translational correction in the partition function becomes in Γ_9 a term $-RT \ln R_i$ for each i chain isolated, or in total:

$$-\phi_0 \sum_{i=1}^{N^*} \phi_i m_i^{-1} P_i \ln R_i \tag{21}$$

Note that the factor ϕ_0, which is almost unity over the experimentally interesting range, is required by thermodynamics, since ΔG must be zero when no solvent is added to the polymer ($\phi_0 = 0$).

IV. Experimental Test of ΔG

1. Comparison with Experimental Data on Polystyrene/Cyclohexane. The ΔG function of eq 10 will be tested against spinodal data, which allow the parameters to be determined satisfactorily by optimization. The validation of the theory is presented first at the crude level which uses standard deviations of least-squares fits in comparison with historical predecessors of the present

Table I
Successive Refinements of the ΔG Function for PS in CH

ΔG function (eq no. for Γ)	sum of squares S, eq 14	σ	β_0	β_1	γ	λ_0[c]	a	T_Θ/K[f]
A. Spinodal Data on 11 Sharp Fractions (cf. Figure 1, Plots 1-11)								
5	3.3×10^{-2}	2.2×10^{-2}	−0.4604	297.30				309.6
6	1.5×10^{-4}	1.5×10^{-3}	0.2654	139.95	0.2952			306.2
7	1.0×10^{-4}	1.2×10^{-3}	0.3074	125.54	0.3033[a]	0.6548		306.0
9	2.6×10^{-5}	6.3×10^{-5}	0.4691	84.89	0.3303[a]	0.6441		306.2
10	1.1×10^{-5}	4.1×10^{-4}	0.1717	100.53	0.4651[b]	0.6215		306.2
B. Spinodal Data on 11 Sharp Fractions and 27 Mixtures (Figure 1, Plots 1-38)								
7	7.9×10^{-4}	1.7×10^{-3}	0.3366	116.74	0.3030[a]	0.5847		306.6
10	3.8×10^{-4}	1.2×10^{-3}	0.2023	91.44	0.4570[b]	0.4879	0[g]	307.9
10[d]	3.3×10^{-4}	1.1×10^{-3}	0.1717	100.53	0.4651[b]	0.6215	0.031	306.2
10[e]	2.0×10^{-4}	8.6×10^{-4}	0.1717	100.53	0.4651[b]	0.6215	0.025	306.2

[a] Theory gives $\gamma = 1/3$ (eq 22). [b] Theory gives $\gamma = 1/2$ (eq 23). [c] Theory gives $\lambda_0 \simeq 0.57$. [d] The sharp-fraction parameters from Table IA were kept constant while optimizing α over the data on the mixtures. [e] M_{z+1} adjusted (cf. section IV.3 and Table III) in plot 27b only, from 1.9×10^6 to 2.0×10^6, and α reoptimized. [f] Measurements give $T_\Theta = 306.4$. [g] α fixed at zero; optimized over β_0, β_1, γ, and λ_0.

theory (eq 4–7). We then inspect the fits in detail in graphical form which brings out the diversity of shapes of spinodal curves of polydisperse samples which the theory can match.

Next we proceed down the list of properties more sensitive than spinodals by confronting the theory with critical point and cloud point data. When we reach second virial coefficients, we are at the limit at which the process of refinement of ΔG by phase equilibrium studies has currently little to offer.

2. Successive Refinements of ΔG, Using Spinodal Data on PS/CH. The improvements in fit achieved by successive refinements of the original Flory–Huggins theory are documented in Table I, using 70 spinodal measurements on sharp fractions of PS in CH and 205 such measurements on mixtures of sharp fractions of PS made over several years by workers in our laboratory (Table II). The standard deviations shown in column 3 refer to the quantity J/RT (eq 11). The five rows in Table IA cover sharp-fraction data only because the first two theories (eq 5 and 6) have spinodals independent of M_z, which would give excessively poor fits to the other experiments. Table IB presents fits of eq 7 and 10 to all (70 + 205 =) 275 data points. The improvement in fit to sharp fractions in Table IA passing down from eq 5 to eq 9 is reflected by the 54-fold decrease in the standard deviation in column 3. This improvement must, of course, be scrutinized in the light of the adjustment of additional parameters. We now show that the degree of this adjustment is not serious since independent theoretical estimates exist for the values of the parameters, and the optimized parameters always (a) lie close to these values and (b) are seen to approach progressively closer as the refinement proceeds down the table.

The Θ temperature of PS/CH, measured to be 306.4 ± 0.2 K, would allow one parameter to be eliminated throughout. Instead we present (column 9) the T_Θ calculated from ΔG with the optimized parameters. The agreement is generally close. The Flory–Huggins model of eq 5 (top line, Table IA) reverts to the original status of a 1-parameter theory. An estimate for λ_0 was given by Koningsveld et al.[7] as 0.57, a value approached proceeding down Table IA better than one ought to expect. Passing to γ, two concordant approaches to its theoretical prediction exist.

(i) Following Kennedy,[23] we make the mild postulate that the critical concentration $\phi_{cr} \to 0$ as $m \to \infty$. From the limiting spinodal and critical point conditions for a monodisperse system, one shows from this postulate:

$$\gamma = 1/3 \quad \text{(for the } \Delta G \text{ function of eq 9)} \tag{22}$$

and

$$\gamma = 1/2 \quad \text{(for eq 10)} \tag{23}$$

Table II
Stated Molecular Weight Average (Samples 1-11) or Calculated Values of Prepared Mixtures (Samples 12-38)

sample no. (Figure 1)	$\bar{M}_n \times 10^{-5}$ (not used)	$\bar{M}_w \times 10^{-5}$	$\bar{M}_z \times 10^{-5}$	$\bar{M}_{z+1} \times 10^{-5}$
1	0.49	0.51	0.55	0.57
2	1.54	1.63	1.81	2.00
3	4.35	5.20	5.90	6.50
4	0.49	0.51	0.55	0.58
5	1.11	1.20	1.29	1.38
6	1.54	1.66	1.81	1.90
7	1.93	2.00	2.07	2.14
8	3.92	4.11	4.31	4.51
9	4.90	5.00	5.93	6.50
10	8.60	8.60	8.62	8.63
11	19.9	26.10	32.20	38.00
12	0.45	1.65	4.32	5.00
13	0.54	1.12	1.72	1.94
14	0.496	2.02	4.45	4.94
15	0.39	1.14	3.77	4.86
16	0.41	1.15	3.18	4.01
17	1.19	1.66	3.95	7.29
18	0.59	4.13	8.21	8.58
19	2.22	4.165	13.15	20.20
20	5.70	5.83	5.96	6.10
21	4.90	4.98	5.93	6.50
22	2.095	3.47	4.50	4.60
23	2.11	5.22	7.89	8.30
24	11.71	13.92	16.24	19.00
25	7.74	12.10	16.75	19.00
26	3.34	11.47	16.90	19.00
27	3.60	12.25	18.92	19.00 (a)
				20.00 (b)
28	1.540	6.720	17.84	19.00
29	0.59	0.76	1.03	1.16
30	0.45	0.76	1.41	1.80
31	0.50	0.77	1.42	2.54
32	3.08	3.44	3.72	3.90
33	2.39	2.67	3.03	3.40
34	2.01	2.44	3.02	3.53
35	0.50	0.78	1.21	1.48
36	3.11	3.39	3.60	3.73
37	0.80	1.10	1.41	1.57
38	1.50	1.65	1.77	1.86

Table III
Molecular Weight Averages for Sample 27

	$M_w \times 10^{-5}$	$M_z \times 10^{-5}$	$M_{z+1} \times 10^{-5}$
(a) reputed	12.25	18.92	19.00
(b) adjusted-see text	12.25	18.92	20.00
	δ_1[a]	δ_2[a]	
(a) mol wt $\times 10^{-5}$	19.00	0.1463	
wt fraction	0.642	0.358	
(b) mol wt $\times 10^{-5}$	20.12	1.865	
wt fraction	0.569	0.431	

[a] Calculated four-equivalent mixture, i.e., two δ-function distributions δ_1 and δ_2 which are calculated to give the same M_w, M_z, and M_{z+1}.

In passing to the limit $m \to \infty$, the dilute-solution term $\phi_0\phi m^{-1}P \ln R$ (in eq 9 or 10) has been set to zero. Accordingly, γ is estimated from the simple Flory–Huggins form of eq 6 with (eq 23) or without (eq 22) the Huggins second-nearest-neighbor correction.

(ii) The lattice theory gives

$$\gamma = 2/z$$

where z is the coordination number. Accordingly, passing from (22) to (23) by introducing the Huggins correction is equivalent to a change from the cubic ($z = 6$) to the tetrahedral ($z = 4$) lattice. This change is not inappropriate for our purpose, since the theory of the partition function of an isolated chain was explicitly illustrated for the tetrahedral lattice. The agreement in column 6 of Table I of the optimized value of γ with eq 22 and 23 is gratifying.

The convergence in successive refinements of empirical parameters upon values derived from theory or experiment, illustrated (Table I) for γ, λ_0, and T_Θ, has its counterpart in the procedure of transforming a constant, derived from theory, into an adjustable parameter u, say. In this way, the factor exp(−1) in eq 18 was transformed into exp(−u), and eq 10 was reoptimized over the spinodal data. The optimized value of u returned was 0.96, close enough to the theoretical value of 1.00 to support the concept which forms the major new and simple element in eq 9. The early theory of eq 6, uncorrected for statistical heterogeneity of semidilute solutions, is recovered by putting $u = 0$. The formal adjustment of u from 1.0 to 0.96 effects a quite negligible reduction in standard deviation by about 1%.

3. Fitting of Spinodal Curves. The curves fitted to spinodal measurements below were calculated from r-equivalent[5] distributions with $r = 2$. In this way, the actual samples were replaced by two delta-function distributions δ_1 and δ_2 (absolutely sharp fractions) of such molecular weights and at such relative concentrations as to keep M_w, M_z, and M_{z+1} invariant. Although some of the mixtures actually employed had three or four components, each representing a rather sharp fraction, there is no point in trying to match averages higher than M_{z+1} at present. Sample computations of the two equivalent δ functions are shown in Table III for sample 27. This sample is referred to again later in this paragraph because its recorded averages M_w, M_z, and M_{z+1} revealed a somewhat pathological pattern, leading to the adjustment shown under (b) in the table. The small adjustment is here seen to lead to a disproportionately large effect on the molecular weight of the lower fraction (δ_2), changing it from 14 600 to 186 000.

Figure 1 contains the 38 plots, with in all 275 measurements of spinodal temperatures T_{sp}, on 11 sharp fractions (plots 1–11) and 27 mixtures of sharp fractions (plots 12–38) of PS, as functions of concentration in CH. Of these, plots 1 and 3 are taken from Scholte's measurements in conventional light-scattering apparatus,[25] the rest being taken with our pulse-induced critical scattering (PICS) apparatus. Some were previously published[5,11] or are taken from the thesis by Derham,[26] but most are new measurements. All the PS fractions used were from Pressure Chemicals. Plots illustrating the Debye–Scholte extrapolation procedure for extracting T_{sp} have been previously published.[27] A typical standard deviation for the experimental error in T_{sp} is about 0.05 K.

The theoretical curves shown are computer plots based on eq 10 with the parameters shown in the legend. Each plot is produced by computation of 75 T_{sp} values and curve fitting by a spline method.

Inspection of the 38 plots for the degree of relative fits achieved must take account of any differences in scale units along both axes from plot to plot. The overall first impression conveyed is of experimental scatter from the theoretical curves by many times the experimental error, and that the deviations in individual plots are not random, but reveal strong systematic errors. These systematic errors arise in large part from inadequate knowledge of the molecular weight averages of the samples. To take a specially marked instance: Plot 1, calculated from the value $M_w = 51\,000$ supplied by the manufacturer, lies well below all measured points. The calculated line for 55 000 lies above the points, and this adjustment is not far greater than the calibration error of M_w. When the individual curves are shifted up or down (along the line joining their maxima to the Θ point, $\phi = 0$, $T_\Theta = 306.4$ K) to compensate for possible systematic errors arising from molecular weight uncertainties, very few of the 275 points lie further than 0.2 K from their curve over the whole 17 degree range covered.

Spinodal measurements can only be made in the neighborhood and on both sides of the critical point, where the metastable range between cloud point and spinodal is not too large, because the Debye–Scholte extrapolation becomes unduly long and inaccurate whenever the metastable range is large. Now the critical point lies at the maximum in solutions of homodisperse polymers, and close to the maxima with the sharp fractions tested (plots 1–11). In the remaining plots, based on mixtures of fractions, the critical points must lie on the descending branch,[28] and this explains the location of the experimental points in plot 12, say, (mixture) compared to plot 10 (sharp fraction). Altogether, a variety of observed shapes are remarkably well reproduced by the theory; contrast especially the convex and highly asymmetric plot 3 with the concave plot 17. The differences between these plots have a simple source.

Homodisperse fractions produce convex and highly unsymmetric forms which have been qualitatively understood for over 40 years. A mixed solution of two such fractions does not produce a spinodal plot remotely like a linear interpolation between those of solutions of the two fractions measured separately. The reason for this nonlinear behavior is straightforward: fractionation of molecular weights cannot occur in a homodisperse solution, but it markedly influences the free energy of mixing a heterodisperse solution, frequently producing spikes on measured cloud curves, and also on the spinodals we calculate here. The points in plots 17, 26, and 25 also give a little experimental support to spikes in the spinodal plots at low concentrations, but in plot 20 they clearly do not match the spike on the theoretical curve.

Table IV
Critical Points Calculated from Equations 7 and 10 (α = 0 in Eq 9) and Data from Koningsveld, Kleintjens, and Schultz[29]

sample no.	mol wt av × 10^{-3}			experiment		equation 7		equation 10 (α = 0)	
	$\bar{M}_w$	$\bar{M}_z$	$\bar{M}_{z+1}$	ϕ_{cr}	T_{cr}	ϕ_{cr}	T_{cr}	ϕ_{cr}	T_{cr}
1	35	46	59	0.135	284.60	0.144	285.00	0.147	284.54
2	51	55	59	0.109	288.85	0.112	289.09	0.106	288.57
3	62	71	81	0.107	290.45	0.108	290.63	0.107	290.02
4	93	96	99	0.087	293.65	0.086	293.62	0.079	293.07
5	166	181	197	0.073	296.60	0.071	296.80	0.073	296.22
								(0.040)[a]	(297.00)[a]
6	286	438	671	0.070	298.70	0.069	298.71	0.099	297.91
								(0.094)[a]	(297.79)[a]
7	394	423	454	0.051	300.70	0.049	300.13	0.056	299.68
8	527	593	667	0.047	301.15	0.045	300.90	0.059	300.51

[a] α fixed at 0.028.

The occurrence of these spikes, and the whole course of the spinodal curves especially at and beyond the lowest concentrations in the plots, becomes progressively more sensitive to parameters, especially to α. In addition, there is the sensitivity to the molecular weight averages M_w, M_z, and M_{z+1} of the sample. In particular, for samples of high molecular weight, which are nearly homodisperse, the data can generally be well fitted by assuming $M_w = M_z = M_{z+1}$. If the polydispersity *is* taken into account, by raising M_z and M_{z+1} somewhat above M_w, the fit can be improved without undue sensitivity to the absolute values of M_z and M_{z+1} but their ratio M_{z+1}/M_z is very critical. The combination $M_w < M_z = M_{z+1}$ is mathematically forbidden, there being no distribution compatible with it. Accordingly, if we adjust $M_w < M_z$, and $M_z \rightarrow M_{z+1}$, some singular behavior in the spinodal is to be expected. It comes about because the equivalent distribution of two δ functions used to compute the spinodal will comprise one δ function of extremely low molecular weight in substantial proportion, and the spinodal at low concentration is exceedingly sensitive to low molecular weights.

The optimization of parameters over the 38 plots was carried out objectively by calculating all the values of M_z and M_{z+1} from the rough data generally available. The only exception is plot 27b, which differs from 27a by adjustments in M_z and M_{z+1} which are quite arbitrary but well within present limits of accuracy of any experimental check. it was noted that the original estimates of M_w = 1.225, M_z = 1.892, and $M_{z+1} = 1.9 \times 10^6$ were unrealistically close to the singular case $M_w < M_z = M_{z+1}$ just mentioned, and that the resulting plot 27a accounted for about half of the total variance due to all errors in the 38 plots. When the adjustments M_z = 1.8, M_{z+1} = 1.9, or M_z = 1.9, M_{z+1} = 2.0×10^6 were made, the calculated spinodals gave satisfactory plots, indistinguishable from each other on the scale shown, designated as 27b. The σ value of the overall fit over 38 plots is reduced from 1.1×10^{-3} to 8.6×10^{-4} by substituting 27b for 27a (bottom of Table IB).

A further systematic trend underlying the overall variance is important. The 275 experimental points shown include 37 points above 301 K, and *all* of these lie *above* their calculated spinodals. These points refer to samples of high molecular weight and contain various proportions of one high molecular weight fraction available. The explanation of the systematic error must be that this high molecular weight sample in our experiments had a substantially higher molecular weight than assumed. The alternative explanation, that our ΔG function is faulty for high molecular weight samples, is not plausible, because the Θ point, corresponding to MW = ∞, is calculated at 306.2 K, in excellent agreement with the accepted experimental value 306.4 K. It would be unsafe to attempt correction by way of optimizing the fit through adjustment of the high molecular weight sample. Instead we accept our optimized parameters (legend of Figure 1) as adequate.

4. The Polydispersity Parameter α. Increasing values of the parameter α in eq 9 progressively raise ΔG and raise the spinodal plots toward higher temperature especially at low ϕ. In a binary mixture of two sharp fractions differing in chain length by a factor f, the correction of $+RT$ in ΔG, for each mole of isolated chains (section III.1), is modified by α: the nonoverlapping smaller chains attract an additional penalty in ΔG of $^1/_2\alpha(\ln f)RT$ per mole while the nonoverlapping longer chains are each favored by $-^1/_2\alpha(\ln f)RT$. The optimized value of α (Table IB) is about 0.03, so that, even for a ratio of f = 100, the correction amounts to only $\pm 0.07RT$ for a mole of isolated chains. For comparison, the total Γ contribution incorporated in ΔG is approximately $2^{-1}mRT$ per mole of chains, where the chain length $m \sim 10^4$ for molecular weight $M = 10^6$. A detailed theoretical analysis of the meaning of α is hardly, therefore, to be sought. The parameter would contain corrections for deviations from the spherical shape of the isolated coils. In addition, differential deviations from athermal mixing for chains of different sizes may be involved. On diluting a solution of a homodisperse polymer, the neglected enthalpy change attending the emergence of a chain into a state free from overlaps will be compensated by adjustment in λ_o. The same applies to the equally neglected and concomitant contraction in coil volume in the same process, as discussed in section V.5. The minuteness of the α correction for differential effects due to polydispersity makes it difficult to explain even its observed sign at present. Though the correction of the ΔG function for statistical heterogeneity in homodisperse polymers is itself small, being RT per mole of isolated chains, it renders the ΔG function enormously more sensitive, in the vicinity of the critical point, to further corrections like that for heterogeneity. This is rationalized below in section V.4 because of the cardinal transformation of the virial series by the Poisson exponential factor which specifies the fraction of chains isolated.

5. Fitting of Critical Point Data. The availability of new computer programs based on r equivalence and eigenvalue methods[5] enables us to present fittings of critical point data published in 1970 by Koningsveld and co-workers.[29] Table IV shows that, with the parameters determined by spinodal measurements (Table I), the preaveraged bridging function eq 6 fits these as closely as one could hope and often within experimental error. Since the critical point condition involves third-order differentials of ΔG, and spinodals only second order, one would expect critical points to be harder to fit to theories generally, but this is not found to be the case. It is, however, understandable that polydispersity has more serious effects on spinodal curves because fractionation, which is absent

at the critical point, becomes progressively stronger as we move along the spinodal away from that point. The refinement of the ΔG function in passing from eq 7 to 10, which substantially improves the fit to spinodal data (Table I), leads to an unmistakable deterioration of the overall fit of the critical point data (Table IV). The most likely cause lies in the truncation, which is rigorous only for eq 7, implicit in the replacement of the molecular weight distributions by δ functions. The truncation theorem[5,13] for spinodals demands two δ functions in the case of eq 7 and for critical points the use of three δ functions for complete rigor. Five moments determine the critical point for eq 7, including $M_0 = \phi$ (eq 12), which the experimenter controls through the polymer concentration. The moments M_1 to M_4 can be calculated from a knowledge of $\bar{M}_w$, $\bar{M}_z$, $\bar{M}_{z+1}$, and $\bar{M}_{z+2}$, but we lack knowledge of $\bar{M}_{z+2}$ from experiments. Accordingly, $\bar{M}_w$, $\bar{M}_z$, and $\bar{M}_{z+1}$ were used for computing merely two equivalent δ functions, thus undercutting the strictly valid truncation limit. This amounts to accepting for $\bar{M}_{z+2}$ the value implied by the calculated mixture of two δ functions. The adequacy of this overtruncation is demonstrated by the excellent fits of ϕ_{cr} and T_{cr} for eq 7 in Table IV. For eq 10, no strict limit applies to the number of moments required. This is because the function Γ_{10} is not formally expressible as a function of a finite set of moments (cf. eq 12). Undoubtedly the effect of higher moments will in practice decrease rapidly, especially for spinodals, and less rapidly for critical points, which require 3/2 times more moments than spinodals when truncation does apply.[5,13] We do observe that eq 10 improves the fit of spinodals in comparison with eq 7 (Table I) but fits critical points a little less well (Table IV), though still very adequately. The general success in predicting critical volumes and temperatures, using parameters calibrated in advance, especially with the theory of eq 7, is further solid support for the notion of refining the Flory–Huggins theory by allowing for statistical heterogeneity in dilute solutions.

6. Fitting of Cloud Point Data. The theoretical model, embodied in the ΔG function of eq 10 with the parameters preoptimized to fit the 275 spinodal points in Figure 1, as listed in the legend, was tested against recent cloud point measurements by Nakata et al.[30] The cloud point equation, even for the case of a homodisperse solution, is analytically complex and very laborious to solve by computer. The computed range is plotted in Figure 2 together with the data. The molecular weight M of the PS used was stated to be 1.56×10^6, the measured T_{cr} to be 303.65 K, and ϕ_{cr} to be 0.0322. Figure 2 shows curve b, matching the stated M, and curve c, matching the experimental T_{cr}. In neither case (see legend) does $\phi_{cr,calcd}$ fit well. The systematic displacement of the theoretical plots from the highly precise data mirrors the kinds of displacement of most spinodal curves (Figure 1) employed in optimizing the parameters in the free energy function. Again some displacement is inevitably due to the errors in calibrating molecular weights, as gauged by comparing plots b and c. The displacement from the data of curve b amounts to only 0.05° at its lower end and to 0.90° at the upper end. We are not dismayed at the magnitude of these displacements for the present stage of refinement of ΔG, considering that Figure 2, without adjustment, tests the parameters determined from spinodals against measurements of cloud points, which are much more sensitive, especially to higher moments of the molecular weight distribution. We are gratified that the shapes of plots b and c do mimic well the experimental curve, not only in slope but in curvature.

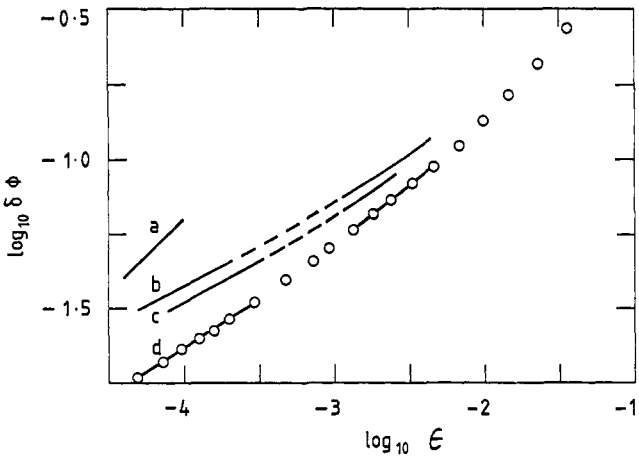

Figure 2. Conventional double logarithmic plot of log $\delta\phi$ against ϵ ($=(T_{cr} - T)T_{cr}^{-1}$) of the cloud point curve. (a) Line of slope $^1/_2$ for comparison, being the asymptotic slope of curves b and c at $-\infty$. (b) Cloud point curve calculated from the theoretical ΔG function (eq 10 with $\alpha = 0$ in eq 9). The parameters β_0, β_1, γ and λ_0 are taken from the optimization for spinodal data, Table IA, row 5, and Figure 1. Assumed $M = 1.56 \times 10^6$. Calculated $\phi_{cr} = 0.0342$, $T_{cr} = 302.96$ K. Mean shapes of solid portions of calculated curve (which simulate the critical exponent): 0.276 (left), and 0.336 (right). (c) Same as (b), but using $M = 2.5 \times 10^6$. Calculated $\phi_{cr} = 0.0295$, $T_{cr} = 303.65$ K. (d) Experimental data by Nakata et al.[30] Mean slopes of solid portions 0.324 (left) and 0.405 (right). $\phi_{cr,exp} = 0.0322$, $T_{cr,exp} = 303.65$ K.

The situation revealed by Figure 2 is just the reverse of that traditionally found in fitting mean field theories to data of this kind.[31,32] Traditionally, mean-field theories fit measurements quite well at high ϵ, but at low ϵ the approach to their inevitable high limiting slope of $^1/_2$ has produced marked deviations from data well within the accessible range. Theoreticians tend to attach great significance to matching the limiting $\epsilon \simeq 0.32$ of the Ising model, which does not use the mean-field approximation. For the first time, we show a mean-field calculation which produced slopes slightly *lower* than that of the experimental line over the whole range accessible both to present-day experiment and to present-day computation. We have not estimated how closely one must approach to $\epsilon = 0$ before the limiting slope of $^1/_2$ is substantially and finally approached. Figure 2 shows that it occurs at a temperature less than 0.015° from T_{cr}. This underlines our previous warnings,[33] based on calculated spinodal lines, against accepting experimental plots such as *d* as evidence for the superiority of three-dimensional Ising-type models over the graph-like-state mean-field concept.

V. Discussion

1. Effects Neglected in the Theory for ΔG. Having described the present theory and its testing against a substantial body of data, we turn to what it leaves out of consideration in order to assess the likely path of future refinements.

2. Approximate Treatment of Fluctuations. The refinement consisting of the elimination of the mean-field approximation by exact summations based on partition functions for models of *localized* systems, like the Ising model, is left out for good reasons. The importance of fluctuations around the mean, as the critical point is approached, cannot be denied. However, it has emerged that for PS/CH (a nonlocalized system of great mobility) such effects are adequately modeled by the two-phase bridging theory, initiated by Koningsveld et al.,[7] outside the range $T_c - 0.015 < T < T_c + 0.015$ K where no data are available. The tests so far proposed for using exact summations of

Table V
Contributions to, and Sum of, Virial Series (eq 26) for $M = 2.61 \times 10^6$, $T = 303.7$ K[a] (cf. Figure 1, Plot 11)

		$A_i\phi^i$		$\sum_{j=1}^{i} A_j\phi^j$	
i	A_i	$\phi = 0.01$	$\phi = 0.02$	$\phi = 0.01$	$\phi = 0.02$
1	-4.512×10^{-5}	-4.512×10^{-7}	-9.024×10^{-7}	-4.512×10^{-7}	-9.024×10^{-7}
2	5.673×10^{-3}	1.612×10^{-7}	2.269×10^{-6}	1.161×10^{-7}	1.367×10^{-6}
3	-4.057×10^{-1}	-4.056×10^{-7}	-3.246×10^{-6}	-2.895×10^{-7}	-1.879×10^{-6}
4	$1.840 \times 10^{+1}$	1.840×10^{-7}	2.944×10^{-6}	-1.055×10^{-7}	1.065×10^{-6}
5	$-5.750 \times 10^{+2}$	-5.760×10^{-8}	-1.840×10^{-6}	-1.631×10^{-7}	-7.750×10^{-7}
6	$1.344 \times 10^{+4}$	1.350×10^{-8}	8.600×10^{-7}	-1.496×10^{-7}	8.496×10^{-8}
7	$-2.512 \times 10^{+5}$	-2.50×10^{-9}	-3.22×10^{-7}	-1.521×10^{-7}	-2.365×10^{-7}
8	$3.913 \times 10^{+6}$	3.0×10^{-10}	1.00×10^{-7}	-1.518×10^{-7}	-1.364×10^{-7}
9	$-5.22 \times 10^{+7}$		-2.7×10^{-8}		-1.631×10^{-7}
10	$6.103 \times 10^{+8}$		6.0×10^{-9}		-1.569×10^{-7}
			$\Delta\mu_1/RT = \sum_{1}^{\infty} A_j\phi^j$:	-1.518×10^{-7}	-1.580×10^{-7}

[a] Critical point from eq 10: $\phi_{cr} = 0.0290$, $T_{cr} = 303.7$.

localized models, inasmuch as they are based on critical exponents, need extension to cope with the conspicuous experimental effects of polydispersity. The difficulty with testing merely critical exponents lies in the impossibility of verifying *empirically* that experimental data have reached the region where relevant asymptotic slopes have been attained (see Figure 2, line a). By comparison, the refinement of replacing a single mean field by two mean-field phases, which mix athermally (as implied by Poisson statistics), though only a crude first step toward accounting for extensive fluctuations, accommodates polydispersity well and poses no convergence problems.

3. Neglect of Volume Changes on Mixing. Turning to elements of mean-field theories omitted from eq 10, the corresponding-state effects associated with non-zero volumes of mixing are more relevant. These effects are dominant near the lower critical solution temperature, which in PS/CH lies far above the experimental range fitted in this paper. Nevertheless, such effects must be expected to make *some* contribution to ΔG even at much lower temperatures. Kleintjens[34] has shown how such effects can often be modeled successfully by mean-field models of the lattice-gas type. The absence of theoretical parameters reflecting the concentration of "holes", and its role in modeling nonzero ΔV_{mix}, in eq 9 means that such effects are "mopped up" in the remaining small deviations of adjustable parameters from their theoretical values. In particular, the expression $\beta_0 + \beta_1 T^{-1}$, which is featured in our eq 6, 7, 9, and 10, represents a series from which terms of known form[35] have been truncated. The higher terms would inevitably become apparent in ΔG at high temperature, but are found not to be detectable with statistical significance in phase equilibria below T_Θ.

4. Refinements in the Virial Coefficients. In 1976, Kleintjens, Koningsveld, and Stockmayer extended to fractionation data on heterodisperse PS in CH their original theory aimed at allowing for this heterogeneity to fractionation data on heterodisperse systems undergoing phase separation.[36] Such data would be expected to produce a test of rather extreme sensitivity to the form of the free energy function. Accordingly, it does not seem surprising that they found calculated Breitenbach-Wolf plots to give poor fits to experimental data (also on PS/CH). They list four paths for possible further refinement of their theory, of which the first three may be briefly discussed, because their continued neglect in our model theory might be queried. The first two paths reflect on improvements in the second and third virial coefficients.

The original derivation of the convergent partition function for a chain isolated in solution "was in large measure motivated by the obvious need to formulate a partition function for the statistical fraction of isolated chains, which feature in applications "[7,36]" of bridging theory to phase equilibria, so as to free ourselves from the piecemeal ascent through the virial series".[17] The need for this liberation is underlined as a result of the present implementation of the program.

We recall that in the series for the relative chemical potential of the solvent:

$$\frac{\mu_1 - \mu_1^0}{RT} = \sum A_i \phi_i \tag{24}$$

the first virial coefficient A_1 is fixed by thermodynamics to be $-m^{-1}$. This value is also derivable from the Flory–Huggins theory and all its refinements (eq 4, 5, 6, 7, 9, and 10). For A_i with $i \geq 2$, statistical mechanical theories are required. Possible improvements to existing theories for A_2 and A_3 (which practically exhaust the available stock) were discussed by Kleintjens et al.[36] as providing pathways to refinements of their bridging theory. This ascent through the virial series is now shown not to be too fruitful for refining ΔG functions which are to account for phase-change properties in the region of the critical point.

Using the following formula[23] for the A_i

$$A_i = -\frac{1}{i}\left[1 + \frac{1}{(i-2)!}\Gamma^{(i)}(0)\right] \tag{25}$$

we find for Γ_{10}, applied to sharp fractions (with $\alpha = 0$ in eq 9)

$$(i > 2): \quad A_i = -\frac{1 - \gamma^{i-1}}{i} + (i-1)\left[\gamma^{i-2}(1-\gamma) \times (\beta_0 + \beta_1 T^{-1}) + (-1)^i m^{-1}\left\{\frac{(\lambda_0 m^{1/2})^{i-2}}{(i-2)!}\left(1 + \frac{\lambda_0 m^{1/2}}{i-1}\right)\right\}\right] \tag{26}$$

Using the optimized parameters from the fittings of spinodals in Table IA, we show in Table V calculations for the first ten coefficients for the high molecular weight fraction ($M = 2.61 \times 10^6$) at a temperature near its critical point and the corresponding contributions to the virial series at concentrations $\phi = 0.01$ and 0.02, i.e., at the dilute end of the spinodal data in plot 11 of Figure 1. The sums to infinity of the virial series are also tabulated. The table shows that even at a concentration as low as $\phi = 0.01$, the first four virial contributions together fall short by over 30% of the sum of the total series, and for $\phi = 0.02$, the seventh virial term alone is over twice the total sum! In

this situation it is not fruitful to attempt theoretical refinements of the second or third coefficients, A_2 and A_3, in isolation, if our aim is to improve ΔG for fitting phase equilibrium data. Since, in the experimental range, higher coefficients contribute such substantial effects to μ_1, i.e., to the first derivative of ΔG, the same must be true *a fortiori* for spinodals and critical points, which involve the second and third derivatives. Although seven virial coefficients are known for a hard-sphere gas, the prospect of calculating from theory A_7 for polymer solutions are dim.

It was foreseen[17] that the original bridging theory[7] (cf. eq 7) already contained, at least in principle, the desired improvement in formulation of the overall virial series. The present simplified version (eq 10) not only fits spinodal data better, but also renders this aspect transparent. While the original Flory–Huggins theory furnishes a rapidly convergent virial series, with $A_i < 0$ for $i > 2$, Table III shows that the bridging theory (eq 10, $\alpha = 0$) gives an alternating series, which is only slowly convergent in the range accessible to experiments on phase equilibria. This is indeed due to the exponential term $\exp[-\lambda_0 m^{1/2}\phi]$ injected by the Poisson statistics.[7] Physically, this means that the bridging theory injects a transition into the thermodynamic behavior in the concentration range around ϕ^*, here modeled by

$$\phi^* = 1/(\lambda_0 m^{1/2}) \tag{27}$$

where the isolated coils would, if separated, just fill the total volume.[7] We find that generally $0 < \phi^* < \phi_{cr}$. Although the transition injected by the factor $\exp[-\lambda_0 m^{1/2}\phi]$ is not sharp, it inevitably has profound effects on the virial series, and produces marked flattening of spinodal curves especially at high molecular weight (plots 10 and 11 of Figure 1) and marked reductions in the *apparent* critical exponents suggested by plots such as in Figure 2 (but not, of course, on the actual critical exponent of $^1/_2$ given by the theory, in plot 2a).

Needless to say, the refinement of A_2 retains all its interest for measurements of appropriate properties at sufficiently high dilution to render the higher A_i truly harmless. A more detailed analysis of the transition behavior is reserved for future reports.

5. Neglect of Changes in Chain Dimensions. The third suggestion of Kleintjens et al.[36] is to allow for changes in volume of isolated coils through variations of λ_0 (eq 27) as a function of T. It is true that the value of this volume sensitively affects the chance of isolation of a chain by using Poisson statistics; yet λ_0 has been taken as fixed (at $T = T_\Theta$) in their bridging theory and ours.

The following argument plausibly justifies this neglect. The ratio $\overline{R^2}/\overline{R_0^2}$ for a given chain at fixed temperature $T < T_\Theta$ is theoretically predicted to increase with concentration in the range of $0 < \phi > 1$ approaching closely to unity at high concentration. The crude Poisson statistics (eq 20) assign equal $\overline{R^2}$, and therefore equal volume, to all chains at given molecular weight at all temperatures, although the dilute "phase" of isolated chains has virtually $\phi = 0$, while the concentrated "phase" can range to quite high concentrations. Actually, parameter λ_0 will contain the ratio $\overline{R^2}(\text{dil})/\overline{R^2}(\text{conc}) < 1$, and as long as this ratio is approximately constant at different molecular weights and temperatures in the spinodal measurements (Figure 1), the changing chain dimensions will be without effect.

But this constancy of $\overline{R^2}(\text{dil})/\overline{R^2}(\text{conc})$ is plausible *at the critical points* for different samples—just as in corresponding-state theory, many dimensionless ratios are found constant at the gas–liquid critical point. Spinodal measurements are necessarily made in the vicinity of the critical point of each sample; minor *relative* differences in chain dimension are absorbed into an adjustment of λ_0, plus minor adjustments of the other parameters, in the model.

VI. Conclusions

The present work is not concerned with prediction of results of future measurements, nor the determination of optimal values for thermodynamic parameters such as virial coefficients. The work *is* concerned with the validation of a more refined model for the thermodynamic behavior of suitable polymer solutions. Because of the generality of the concepts used in the model, which do not reflect specific properties of PS and CH, one may hope that the form of the ΔG function (eq 10) can be applied generally to nonpolar polymer/solvent pairs whose upper and lower critical solution temperatures are sufficiently widely separated. This is a worthwhile task, calling, as always,[3] for a strategy substantially different from that of data reduction and prediction. The illusory hope of determining accurately the values of individual parameters by this strategy is dashed by a glance at the large *fluctuations* in the values of β_0 and β_1 in Table I under successive refinements going down the table. The statistical coupling under optimization procedures between these parameters is intense.

The nature of the refined bridging (or two-phase) model calls for some comment. It is a nonlocalized model, in which the particle coordinates are randomized in all dimensions but one (in the chain direction) by Brownian motion. This feature characterizes[3] the graph-like state. Although such an essentially one-dimensional theory is crude, it is here shown to fit fairly succesfully spinodals, cloud points, and critical points, including the effects of polydispersity. Indeed, further refinement would seem to hinge largely on better characterization of molecular weights of experimental samples.

Huggins[3] and Flory[2] put forward their famous theory independently. The original second-nearest-neighbor correction of Huggins, already found of some value in an earlier part[39] of this series, really comes into its own in the present work. The correction for statistical heterogeneity of semidilute solutions was essentially developed by the group guided by Stockmayer.[7]

It is pleasant to submit to this anniversary volume, dedicated to Paul Flory, a further attempt at refinement of this correction, to meet a need which he envisaged in his early fundemental contribution to a subject of enduring interest.

Acknowledgment. The Science Research Council is thanked for financial support. Grateful acknowledgement is given to Dr. J. A. Torkington for advice, computations, and critical reading of the manuscript; to Dr. J. W. Kennedy for help with computational techniques and general advice; and to Mr. C. W. R. Sung for some spinodal measurements not previously published.

References and Notes

(1) G. Bachelard, "La Formation de l'esprit scientifique", J. Vrin, Paris, 1970, p 61.
(2) P. J. Flory, *J. Chem. Phys.*, **10**, 51 (1942).
(3) M. L. Huggins, *Ann. N. Y. Acad. Sci.*, **43**, 1 (1942).
(4) T. A. Orofino and P. J. Flory, *J. Chem. Phys.*, **26**, 1067 (1957).
(5) M. Gordon, P. Irvine, and J. W. Kennedy, *J. Polym. Sci., Polym. Symp.*, **61**, 199 (1977).
(6) R. Koningsveld and L. A. Kleintjens, *Macromolecules*, **4**, 637 (1971).
(7) R. Koningsveld, W. H. Stockmayer, J. W. Kennedy, and L. A. Kleintjens, *Macromolecules*, **7**, 73 (1974).
(8) J. W. Breitenbach and B. Wolf, *Makromol. Chem.* **108**, 263 (1967).

(9) B. Chu, F. J. Schoenes, and M. E. Fisher, *Phys. Rev.*, **185**, 219 (1969).
(10) Th. G. Scholte, *J. Polym. Sci., Part A-2*, 1553 (1971).
(11) K. W. Derham, J. Goldsbrough, and M. Gordon, *Pure Appl. Chem.*, **38**, 97 (1974).
(12) J. W. Gibbs, *Trans. Conn. Acad. Arts Sci.*, **3**, 108, 343 (1876/8); reprinted in "The Scientific Papers of J. W. Gibbs", Vol. 1, Dover, New York, 1961.
(13) P. Irvine and M. Gordon, to be published.
(14) P. Irvine and J. W. Kennedy, to be published.
(15) Th. G. Scholte, *J. Polym. Sci.*, **39**, 281 (1972).
(16) P. J. Flory, *J. Chem. Phys.*, **13**, 453 (1945).
(17) M. Gordon, J. A. Torkington, and S. B. Ross-Murphy, *Macromolecules*, **10**, 1090 (1977).
(18) P. J. Flory, "Principles of Polymer Chemistry", Cornell University Press, Ithaca, N.Y., 1953.
(19) A. J. Staverman, *Recl. Trav. Chim. Pays Bas*, **69**, 163 (1950).
(20) P. J. Flory, *Ber. Bunsenges. Phys. Chem.*, **81**, 885 (1950).
(21) J. E. Lennard-Jones and A. F. Devonshire, *Proc. R. Soc. London, Ser. A*, **169**, 317 (1939).
(22) J. Hirschfelder, D. Stevenson, and H. Eyring, *J. Chem. Phys.*, **5**, 896 (1937).
(23) J. W. Kennedy, *J. Polym. Sci. C.*, **39**, 71 (1972).
(24) H. Yamakawa, "Modern Theory of Polymer Solutions", Harper & Row, New York, 1971.
(25) Th. G. Scholte, *J. Polym. Sci., Part A-2*, **9**, 1553, (1971), and ref 7.
(26) K. W. Derham, Ph.D. Thesis, University of Essex, 1975.
(27) H. Onclin, L. A. Kleintjens, and R. Koningsveld, *Makromol. Chem., Suppl.*, **3**, 197 (1979).
(28) H. Chermin, M. Gordon, and R. Koningsveld, *Macromolecules*, **2**, 207 (1969).
(29) R. Koningsveld, L. A. Kleintjens, and A. R. Schultz, *J. Polym. Sci., Part A-2*, **8**, 1261 (1970).
(30) N. Nakata, T. Dobashi, N. Kuwahara, M. Kaneko, and B. Chu, *Phys. Rev. A.*, **18**, 2683 (1978).
(31) P.-G. de Gennes, "Scaling Concepts in Polymer Physics", Cornell University Press, Ithaca, N.Y., 1979, pp 112-123.
(32) N. Kuwahara, J. Kojima, M. Kaneko, and B. Chu., *J. Polym. Sci., Polym. Phys. Ed.*, **11**, 2307 (1973).
(33) M. Gordon and P. Irvine, *Polymer*, **20**, 1449 (1979).
(34) L. A. Kleintjens, Ph.D. Thesis, University of Essex, 1979.
(35) R. Koningsveld, Thesis, University of Leiden, on liquid-liquid phase relationships and fractionation in multicomponent polymer solutions, P. M. Van Hooren, Herleen, 1967, Appendix III. D. Patterson, G. Delmas, and T. Somcynsky, *Polymer*, **8**, 503 (1967).
(36) L. A. Kleintjens, R. Koningsveld, and W. H. Stockmayer, *Br. Polym. J.*, **8**, 29 (1976).
(37) J. W. Kennedy, M. Gordon, and J. W. Essam, "5th Biennial International CODATA Conference Proceedings", Pergamon Press, Elmsford, N.Y., 1977.
(38) M. Gordon, *Polymer*, **20**, 1349 (1979).
(39) M. Gordon, P. Kapadia, and A. Malakis, *J. Phys. A., Math. Gen.*, **9**, 751 (1976).

Notes

Infrared Conformational Study of Poly(ethylene glycol)-Bound Homooligoglycines in the Solid State and in Solution‡

CLAUDIO TONIOLO,[1a] GIAN M. BONORA,[1a]
V. N. RAJASEKHARAN PILLAI,[1b] and
MANFRED MUTTER* [1b]

Biopolymer Research Centre, C.N.R., Institute of Organic Chemistry, University of Padova, 35100 Padova, Italy, and the Institute of Organic Chemistry, University of Mainz, D-6500 Mainz, West Germany. *Received January 23, 1980*

In the light of the recent interest in the investigation of the conformation and conformational stability of biologically active molecules covalently linked to a polymeric support,[2-4] the study of poly(ethylene glycol)-bound polypeptides appears to be of exceptional relevance in many respects. The C-terminal macromolecular protecting group poly(ethylene glycol) (PEG)[5] permits effective stepwise synthesis and allows the conformational investigation of the covalently attached peptide without the time consuming deprotection and isolation steps, due to its favorable physical and optical properties.[6,7] In particular, the strong solubilizing effect of PEG enables conformational studies of the otherwise poorly soluble peptides in a great variety of solvents. Thus, this approach permitted the conformational analysis of homooligomers of L-Ala, L-Val, L-(γ-Bzl)Glu, and L-Met by using CD and IR measurements.[8-13] These results prompted us to extend this approach to the conformational analysis of homooligoglycines. The Gly residue is of particular interest since it can explore a large conformational space, thus inducing a high flexibility to the peptide chain.[14-17] Moreover, the presence of Gly residues induces conformational characteristics in a linear peptide chain which are favorable for cyclization.[18,19]

Experimental investigations of the conformational preferences of monodispersed homooligoglycines were limited to very short chain lengths due to the low solubility of the higher oligomers. In this note we report the IR analysis in the solid state and in solution of a series of PEG-bound homooligoglycines of the general formula *t*-Boc-$(Gly)_n$-OPEG (n = 1-9).

Chromatographically and analytically pure *t*-Boc-$(Gly)_n$-OPEG's up to n = 9 have been synthesized by the liquid phase method[6] by using bifunctional PEG of molecular weight 10 000.

The results of the IR measurements in the solid state are presented in Table I. The assignments of the various bands of these poly(ethylene glycol)-bound peptides were made on the basis of the theoretical and experimental infrared data of peptides and polypeptides. The relative intensities of the bands and their changes with increasing chain length have been taken into consideration in the interpretation of the different bands. When n = 7-9 the peptides assume predominantly the antiparallel β conformation (conformation I).[20] When n = 3-5 the peptides assume a predominant conformation with hydrogen bonds, most probably of the interchain type, but quite different from the usual antiparallel β (conformation I) and ternary helix (conformation II) conformations of poly$(Gly)_n$. In the region of n = 5-7 the antiparallel β conformation adopted by the highest oligomers and the conformation adopted by the lowest oligomers coexist. Contrary to our findings, Ac-$(Gly)_{1-4}$-NHEt's were reported to assume the ternary helix conformation.[21,22] This difference in the conformational preferences of the lowest oligomers can be attributed to the effect of the bulky and bifunctional PEG. To clarify this point, we have carried out the solid-state IR measurements of the low molecular weight analogues *t*-Boc-$(Gly)_{1-3}$-OMe. The IR spectra (Table I) are in reasonable agreement with those of the corresponding Ac-

‡ Dedicated to Professor Paul J. Flory on the occasion of his 70th birthday.

0024-9297/80/2213-0772$01.00/0